



A new method for judging thermal image quality with applications

Sos Aghaian^a, Hrach Ayunts^{b,*}, Thaweesak Trongtirikul^c, Sargis Hovhannisyan^{b,d}

^a City University of New York, New York, 10314, NY, USA

^b Yerevan State University, Yerevan, 0025, Armenia

^c Rajamangala University of Technology Phra Nakhon, Bangkok, 10300, Thailand

^d Institute for Informatics and Automation Problems of NAS RA, Yerevan, 0014, Armenia

ARTICLE INFO

Keywords:

Thermal imaging

Image enhancement

Image quality assessment

ABSTRACT

Infrared thermal imaging, a non-destructive testing technology, measures the surface temperature of objects. Assessing thermal image quality is crucial for image monitoring, system design, algorithm optimization, and benchmarking. However, developing objective metrics that align with human perception is challenging due to the distinct structure of thermal images, which often feature high background temperatures and minimal variance between objects and the background. Existing methods typically target specific local features or overall image contrast, but new measures are needed to bridge the gap between objective performance and the unique characteristics of thermal images.

We propose a novel image quality assessment (IQA) method inspired by the human vision system, specifically designed for thermal images, harmonizing local and global data. The primary contributions include (1) innovative local, global, and hybrid thermal quality assessment methods that deliver precise image quality predictions without needing reference images, (2) an experimental analysis evaluating the developed blind thermal IQA measure's applicability to various thermal images, and (3) a comprehensive analysis of traditional IQA measure-based methods applied to publicly accessible thermal databases. Extensive simulations demonstrate our method's competitive performance and strong alignment with human perception of image quality.

1. Introduction

Thermal infrared thermography (IRT) is a technique that uses thermal cameras to capture images based on the infrared radiation emitted by objects. IRT is a non-invasive diagnostic and monitoring tool with many applications in various industries, such as medical [1,2], defense [3], agriculture [4] and machine industry [5,6]. IRT can be especially useful in traffic and object detection scenarios [7], where the visibility is low due to conditions like nighttime, fog, heavy rain, or smoke. IRT can also help identify abnormal thermal patterns or temperature variations, indicating faults in photovoltaic (PV) modules [8], such as hotspots, cracks, loose connections, insulation breakdowns, or overheating. This can prevent further damage, reduce maintenance costs, and improve efficiency and safety [9]. Moreover, thermal imaging can automatically diagnose diseases and disorders in humans and animals under different environmental conditions. Technological advancements and cost reductions in infrared cameras have made this technique more accessible and applicable to applications previously considered impractical. As a result, IRT has attracted increasing interest from researchers due to its multifaceted applications.

One of the critical challenges in thermal infrared imaging is assessing the quality of thermal images, which can be degraded by various distortions during acquisition, processing, and transmission. Many image processing tools have been developed, focusing on noise reduction or contrast enhancement [10]. These tools aim to measure and improve the quality of processed images. However, blind thermal image quality assessment is challenging, as it requires considering the unique characteristics and diverse applications of thermal images. This assessment is essential for comparing different thermal imaging systems or devices, such as infrared cameras or drones, and selecting the most suitable ones for specific applications or scenarios [11].

Objective quality metrics for image evaluation are categorized as full-reference (FR), reduced-reference (RR), and no-reference (NR). FR image quality assessment (IQA) methods compare an image's quality with a reference image, while NR or blind methods do not rely on a benchmark image [12]. However, due to their distinct structural characteristics, NR-IQA methods typically used for visible light images may not be suitable for thermal images. Some blind IQA methods use artificially generated pseudo-reference images for quality assessment [13,

* Corresponding author.

E-mail address: hrach.ayunts@ysu.am (H. Ayunts).

<https://doi.org/10.1016/j.sigpro.2024.109769>

Received 26 June 2024; Received in revised form 7 October 2024; Accepted 30 October 2024

Available online 7 November 2024

0165-1684/© 2024 Elsevier B.V. All rights are reserved, including those for text and data mining, AI training, and similar technologies.

[14]. Another study introduces a wavelet-predominant algorithm for evaluating the quality and usability of non-visible spectrum THz security images [15]. The latest work includes RichIQA, a novel IQA method that utilizes a three-stage prediction network powered by a Convolutional vision Transformer and a multi-label training strategy [16]. Additionally, there has been a significant advancement in IQA for videos [17].

Pioneering works such as Lifelong Blind Image Quality Assessment (LIQA) by Liu et al. [18] and attention-based neural networks in IQA [19] have improved the accuracy of these methods by focusing on visually significant regions within images. Despite the success of traditional blind IQA methods for visible light images, their effectiveness for thermal images is limited due to essential structural differences. Popular no-reference quality metrics such as BRISQUE, NIQE, and PIQE [20–22], based on natural scene statistics (NSS) [23], MANIQA [24] and TOPIQ [25], leading neural network-based NR-IQA methods, demonstrate the advancements in this field.

Computer simulations show a growing gap between perceptual quality and evaluation results for thermal images, indicating the need for objective metrics aligned with human perception. Also, there is a lack of diversity and annotation in thermal image datasets for given applications, which impacts the robustness and generalizability of quality measures. The single thermal image quality assessments such as EME [26], DMTE, DIMTE, and MDIME metrics [27], and BDIM [28] metrics use human visual system attributes to evaluate thermal image quality. Nevertheless, these methods face challenges in accurately identifying distortions in thermal images, such as noise and blur. Current thermal image quality measures mainly target specific local features within confined areas. While global metrics highlight overall image contrast, they may neglect intricate details. Conversely, local metrics can overlook the comprehensive image context and fail to account for certain distortions characteristic of thermal images.

Given the unique challenges of thermal imaging technology, such as the high background temperatures, minimal variance between objects and the background, and the scarcity of methods explicitly designed for thermal applications, new measures are needed to bridge the gap between objective representation performance and the inherent characteristics of thermal images. These challenges may revolve around answering the following critical questions: How well can conventional visual IQA methods evaluate thermal image processing algorithms? How closely do these methods reflect the human perception of quality in thermal images? How can they be applied in other infrared thermography (IRT) applications?

This paper addresses these challenges by introducing a novel thermal image quality assessment method that combines local and global analysis for accurate image quality predictions without reference images. Our study's main contributions are:

1. **Blind Single Thermal Image Quality Measures:** We develop local, global, and combined metrics for assessing thermal image quality.
2. **Strong Correlation with Mean Opinion Score (MOS):** The proposed methods correlate well with MOS and work effectively under various experimental conditions, including image enhancements and thermal image distortions like noise and blurring.
3. **Thorough Evaluation of Existing Metrics** on publicly accessible databases, including solar panels, thermal images of industrial equipment (such as Induction Motors and Transformers), and multispectral object detection datasets: We perform both qualitative and quantitative evaluations of current thermal image quality metrics using real-world images, including photovoltaic systems, motors, and vehicles. Our approach has proven highly effective, aligning with human perception of a good image. Additionally, we investigate the correlation between our quality assessments and human ratings using thermal image databases, showcasing the efficacy of our approach.

The paper is organized as follows. Section 2 introduces related works on thermal image quality assessment. Section 3 describes the details of the presented method. Section 4 gives computer simulation results and analysis. Finally, Section 5 concludes the work.

2. Related work

Image quality assessment (IQA) is a critical issue in image processing, with applications across various domains [29,30]. As mentioned above assessing image quality is essential for image restoration, compression, transmission, and decolorization tasks. A complete list of NR thermal image quality assessment techniques and their definitions is provided in Table 1. Studies indicate that developing and implementing thermal image quality measures presents several challenges due to thermal imaging technology's unique characteristics and complexities. Key challenges include:

- The difficulty of obtaining reliable ground truth references for thermal images prevents direct comparison and assessment of quality.
- The influence of subjective human perception on thermal image quality assessment can vary among observers due to different criteria, expertise, environmental factors, and application contexts, which highlights the necessity of using opinion score distribution [31,32].
- The challenge of accurately quantifying the temperature variations in thermal images requires careful calibration.
- Thermal images have lower contrast and fewer details than visible-light images, which challenges the assessment of sharpness and clarity. Existing quality metrics for visible-light images may not apply to thermal images.
- Thermal imaging is sensitive to environmental conditions such as ambient temperature, humidity, and the distance from the object being imaged. Integrating these variables into quality assessment is complex but essential for accurate evaluation.
- Thermal images can be affected by various types of distortions, including Gaussian noise, Poisson noise, salt-and-pepper noise, and blurring [23,33]. These distortions can arise from sensor imperfections, electronic interference, environmental conditions, or limitations in the imaging system. Addressing these issues is crucial for ensuring the accuracy and reliability of thermal imaging applications.
- There are few thermal image assessment algorithms, such as EME, DMTE, DIMTE, and MDIME [27], compared to visible light image assessment algorithms, such as BRISQUE, NIQE, PIQE, and others. This limits the choice and comparison of different thermal image quality measurement methods.

To address these challenges, robust approaches tailored to the unique characteristics of thermal images are needed. These approaches should include both local and global measures of the image. Local measures evaluate the quality of specific regions or features within the image, while global measures consider the overall quality of the entire image. Combining local and global measures enables a comprehensive evaluation of the image's fidelity and utility for specific applications. Moreover, developing a thermal image quality measure involves designing suitable algorithms or models that capture relevant features, analyze statistical properties, or consider human perceptual factors. The measure should be robust, computationally efficient, and correlate well with human subjective evaluations or ground truth references.

3. Proposed thermal image quality metrics

This section introduces new metrics designed to evaluate both local and global quality aspects of thermal images, along with a combined metric for comprehensive assessment. As previously noted, traditional no-reference image quality metrics like BRISQUE and NIQE, primarily

Table 1
Summary of previous studies on thermal and related image quality assessment.


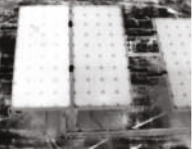


Measure	Definitions
EME [26]	<p>Measure of Enhancement (EME) measures the contrast based on modified Weber's law, which is defined as the average of the local maximum and minimum grayscale intensities ratio in each sub-block.</p> $\text{EME}(I) = \frac{1}{M \times N} \sum_{i=1}^M \sum_{j=1}^N 20 \log \left(\frac{[I_{\max}]_{i,j}^{m,n}}{[I_{\min}]_{i,j}^{m,n} + c} \right) \quad (1)$ <p>where $[I_{\min}]_{i,j}^{m,n}$ and $[I_{\max}]_{i,j}^{m,n}$ denote the local minimum and maximum intensity level in each $m \times n$ local block. c represents a constant to avoid the calculation error due to a logarithmic operation.</p>
DMTE [27]	<p>The measure is based on the integration of the human visual system and a density-based measure.</p> $\text{DMTE}(I) = \frac{1}{M \times N} \sum_{i=1}^M \sum_{j=1}^N \frac{[p_D]_{i,j}^{m,n}}{[p_B]_{i,j}^{m,n}} \log \left(\frac{[p_D]_{i,j}^{m,n}}{[p_B]_{i,j}^{m,n}} \right) \quad (2)$ <p>where $[p_D]_{i,j}^{m,n}$ and $[p_B]_{i,j}^{m,n}$ are the local darkness and brightness density in each $m \times n$ local block. P_a is a probability density function.</p> $[p_D]_{i,j}^{m,n} = \sum_{a=1}^m P_a \div \sum_{a=1}^m [p_B]_{i,j}^{m,n} = \sum_{a=1}^m P_a \div \sum_{a=1}^m P_a \quad (3)$
DIMTE [27]	<p>This measure is based on integrating both the intensity and density of an image. This measure includes features, a human visual system, an information system, and a distribution-based measure.</p> $\text{DIMTE}(I) = \frac{1}{M \times N} \sum_{i=1}^M \sum_{j=1}^N \frac{[p_D]_{i,j}^{m,n}}{[p_B]_{i,j}^{m,n}} \cdot \left(\frac{[I_{\max}]_{i,j}^{m,n}}{[I_{\min}]_{i,j}^{m,n}} \right)^2 \quad (4)$ <p>where $[I_{\min}]_{i,j}^{m,n}$ and $[I_{\max}]_{i,j}^{m,n}$ denote the local minimum and maximum intensity level in each $m \times n$ local block.</p>
MDIMTE [27]	<p>This measure is a local contrast measure of enhancement. It is constructed based on DMTE, DIMTE, and EME measures.</p> $\text{MDIMTE}(I) = \frac{1}{M \times N} \sum_{i=1}^M \sum_{j=1}^N \frac{[p_D]_{i,j}^{m,n}}{[p_B]_{i,j}^{m,n}} \left(\frac{[I_D]_{i,j}^{m,n}}{[I_B]_{i,j}^{m,n}} \right)^2 \quad (5)$ <p>where $[I_D]_{i,j}^{m,n}$ and $[I_B]_{i,j}^{m,n}$ represent the local darkness and brightness intensity level, respectively.</p>
BDIM [28]	<p>Block Distribution-Based Information Measure (BDIM) is a thermal image quality metric based on Human Visual System (HVS) attributes such as local resolution, contrast, and sharpness.</p> $\text{BDIM}(p, I) = \frac{1}{M \times N} \sum_{i=1}^m \sum_{j=1}^n \frac{1}{\left(\frac{[p_{\min}]_{i,j}^{m,n}}{[p_{\max}]_{i,j}^{m,n}} \right) \left(\frac{[I_{\min}]_{i,j}^{m,n}}{[I_{\max}]_{i,j}^{m,n}} \right)^2 + c} \quad (6)$ <p>where p_{\min} and p_{\max} respectively denote the minimum probability density value and the maximum probability density value in each local tile $[m, n]$, $[I_{\min}]_{i,j}^{m,n}$ and $[I_{\max}]_{i,j}^{m,n}$ represent the minimum intensity value and the maximum intensity value in each local tile $[m, n]$, respectively, and c refers to an offset value</p>
BRISQUE [20]	<p>The Blind or no-reference Image Spatial Quality Evaluator (BRISQUE) is a model trained using a database of images that have known distortions, which limits its ability to evaluate images with different types of distortions. Additionally, BRISQUE is designed to be opinion-aware, as it relies on subjective quality scores that are associated with the training images.</p>
NIQE [21]	<p>Natural Image Quality Evaluator (NIQE) is a quality evaluator that uses a database of pristine images for training but can still measure the quality of images with arbitrary distortion. It is designed to be opinion-unaware and does not rely on subjective quality scores.</p>
PIQE [22]	<p>The Perception-based Image Quality Evaluator (PIQE) method is an unsupervised and opinion-unaware algorithm that does not rely on a pretrained model to evaluate image quality. It can assess the quality of images with arbitrary distortion. PIQE approach estimates distortion in individual blocks of the image and calculates the quality score based on the local variance of perceptibly distorted blocks.</p>
MANIQA [24]	<p>MANIQA, or Multi-dimension Attention Network for NR-IQA, is a metric designed to improve the accuracy of assessing image quality, particularly for GAN-based distortion. It utilizes ViT for feature extraction and introduces attention mechanisms (TAB and SSTB) to enhance global and local interactions.</p>
TOPIQ [25]	<p>TOPIQ is an IQA method inspired by the global-to-local processing mechanisms of the human visual system, emphasizes the crucial role of semantic information in guiding the perception of local distortions. TOPIQ utilizes a heuristic top-down network called the Coarse-to-Fine Network (CFAN), which propagates multi-scale semantic information to lower-level distortion features. Essentially, this approach leverages high-level semantics to guide the IQA network, allowing it to focus on semantically significant regions of local distortion.</p>

trained on natural color images, often fail to assess contrast enhancement in thermal imagery accurately. Table 2 illustrates the performance of different image quality metrics in evaluating original and contrast-enhanced thermal infrared images. BRISQUE and NIQE metrics, which generally favor images with lower scores, surprisingly identify the original images (a, c) as having higher quality than their contrast-enhanced counterparts (b, d). In contrast, the LGTA metric, where higher scores indicate better quality, accurately recognizes the superior quality of the contrast-enhanced images. This alignment with human visual perception suggests that LGTA is more robust regarding the effects of contrast enhancement and better captures the perceptual benefits of this image-processing technique. This makes it a valuable tool for evaluating image enhancement techniques' effectiveness and optimizing image processing workflows in applications where visual clarity and information content are critical. A subsequent section will discuss the LGTA metric in more detail, including its underlying principles and advantages over traditional metrics in the context of TIR image analysis.

Typically, thermal image quality measures assess the clarity and contrast within small blocks within an image. These measures consider the combination of these factors to evaluate the overall quality of thermal images. It is important to note that some state-of-the-art metrics, such as BDIM and DMTE, mainly operate as local metrics, relying heavily on the intensity information within blocks of the image. In contrast, recent NR image quality metrics, exemplified by MANIQA, adopt a more holistic approach by integrating both local and global features using transformers and attention mechanisms, thereby achieving superior performance. While effective in some scenarios, these metrics may overlook the impact of various thermal image distortions, such as noise introduced during image acquisition (e.g., sensor limitations or environmental factors). The necessity for specific metrics in the thermal imaging domain is highlighted by challenges related to the shortage of datasets, particularly those lacking perceptual scores for Thermal IQA. These challenges include varied distortions and restricted availability. Under such circumstances, current measures might not provide thorough insights into the quality of thermal images, highlighting the need

Table 2

Comparison of BRISQUE, NIQE, and LGTA metric on thermal images and their enhanced versions. Note: Higher values of LGTA indicate better quality, while the opposite is true for BRISQUE and NIQE.

				
	(a)	(b)	(c)	(d)
BRISQUE	28.085	29.266	29.495	33.356
NIQE	4.8907	4.9074	5.6617	5.9774
LGTA	1.069	1.2879	1.139	1.2478

for more versatile and robust metrics explicitly designed for thermal imaging.

We present new metrics for both local and global quality assessment of thermal images and the combined metric.

3.1. Local and global thermal IQA

The local thermal quality metric is determined through the following steps:

1. The image is divided into k-by-k blocks.
2. The equations presented below are applied to these blocks using block-dependent local mean thresholds.

$$a' = \left(\frac{[\max(I_L)]^{m,n} + 1}{[\min(I_L)]^{m,n} + 2} \right)^\gamma; I_L = \{I_{i,j} \mid I_{i,j} \leq x_\tau\} \quad (7)$$

$$b' = \left(\frac{[\max(I_U)]^{m,n} + 1}{[\min(I_U)]^{m,n} + 2} \right)^\gamma; I_U = \{I_{i,j} \mid I_{i,j} > x_\tau\} \quad (8)$$

$$b_{m,n} = b' \cos(\log(\log(b' + 1)) + 1)$$

where x_τ is the mean pixel value of the (m,n) block, γ is a parameter (for example, $\gamma = 1$, $\gamma > 1$ or $\gamma < 1$), and $\max()$ ($\min()$) function calculates the third maximum (minimum) value in the block if possible.

3. The Local Thermal Assessment (LTA) is then computed:

$$LTA = \frac{1}{M \times N} \sum_{m=1}^M \sum_{n=1}^N (a_{m,n} + b_{m,n}) \quad (9)$$

Motivation for Introducing the Local LTA Measure: Capturing local variations and subtle details is crucial for accurate quality assessment in thermal image analysis. Traditional global metrics often overlook these nuances, leading to potentially misleading evaluations. To address this, we introduce the LTA metric, designed to provide a fine-grained image quality assessment by focusing on local image characteristics. Key Features of LTA:

- LTA utilizes the ratio of the third highest and lowest intensities (3rd-order statistic) within each image block. This approach minimizes the influence of noisy pixels, ensuring a more reliable assessment, particularly in scenarios where noise is prevalent. This strategy aligns with the modified Weber's law principles, which account for the human visual system's sensitivity to relative intensity differences [34].
- LTA employs adaptive thresholding to enhance further noise resilience. Pixels within each block are categorized into two groups (I_L and I_U) based on their mean values, creating dynamic thresholds that adjust to the local image content.

- The LTA metric prioritizes evaluating local features within thermal images. Analyzing intensity variations within individual blocks captures subtle details and textures that global metrics might overlook.
- Mathematical Formulation: The LTA metric incorporates a cosine function transformation to map the intensity ratios to a perceptual quality scale. This transformation, represented by a' and b' , is then calculated by multiplying the ratio by $\cos(\log(\log(\text{ratio} + 1) + 1))$, ensuring that the metric aligns with human visual perception, where small intensity differences are more noticeable in darker regions. The function is key in bridging raw intensity data with human perception in thermal image quality assessment. It introduces non-linearity to mimic human visual sensitivity, making subtle differences in darker regions more noticeable and enhancing the perceptual relevance of thermal images. Additionally, by compressing intensity values, the function reduces the influence of noise and highlights local features, ensuring a more accurate and robust evaluation of image quality.

Fig. 1 illustrates how the LTA metric highlights local features and variations, providing a more nuanced understanding of image quality than global metrics. LTA enables a more accurate and comprehensive evaluation of thermal image quality by emphasizing subtle details, reducing noise impact, and focusing on local features.

We also present a novel parameter-independent Global Thermal Assessment (GTA) quality metric:

$$NS = \frac{std(I_s)}{(1 + |std(I_s) - std(I)|)} \quad (10)$$

$$GTA = \frac{NS}{\sum_{i=1}^M \sum_{j=1}^N p_{i,j} \log_2 \left(\log_2 \left(\frac{p_{i,j}}{p_i p_j} + 1 \right) + 1 \right)}$$

where p_i , p_j , and $p_{i,j}$ are the pixel's probability mass function (PMF) values in the current row, column, and whole image, respectively. The NS quantifies the noise level in the image, where $std(I_s)$ represents the standard deviation of the smoothed image I_s , and $std(I)$ represents the standard deviation of the original image I . Our experiments employ an edge-preserving bilateral filter to smooth the image. However, it is worth noting that other smoothing algorithms, such as median filtering or Gaussian blur, can also be utilized for faster execution when required. The choice of smoothing technique may depend on the specific application and computational considerations.

Motivation for Introducing the GTA Measure: The GTA measure comprehensively evaluates image quality by integrating 2D image histograms with column-wise and row-wise histograms. The 2D histogram captures the overall intensity distribution, while the column-wise and row-wise histograms reveal spatial variations, enabling a deeper understanding of image quality by considering global characteristics.

This method is robust to spatial shifts and rotations, common challenges in image analysis because including column-wise and row-wise

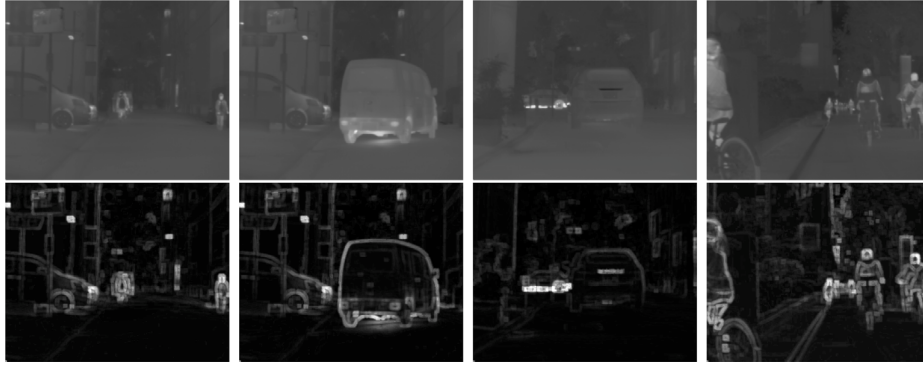


Fig. 1. Visualization of the LTA metric without averaging. The first row shows the original thermal images. The second row displays the images of normalized pixel values used in the metric calculation. It illustrates how the LTA metric highlights local features and variations, providing a more nuanced understanding of image quality than global metrics.

histograms mitigates the sensitivity of traditional 2D histograms to such transformations. GTA's enhanced sensitivity to specific image degradations—such as blur, noise, and contrast distortions—is particularly valuable for thermal imaging, which often involves unique image characteristics and degradations. Its adaptability to detect these nuances makes GTA an effective tool for quality assessment in thermal imaging applications.

3.2. Combined thermal IQA

To incorporate the thermal image's local and global features, we define a combined Local and Global Thermal Assessment (LGTA) metric as a linear combination of LTA and GTA.

$$LGTA = \alpha \cdot LTA + \beta \cdot GTA \quad (11)$$

where α and β are parameters indicating the relative importance of local and global metrics in the combined LGTA metric. By default, both parameters are set to 0.5, reflecting an equal weighting of local and global metrics. However, they can be optimized based on specific image characteristics and classes, allowing for tailored adjustments to suit different image types and applications.

The monotonic nature of a quality metric is a crucial attribute, meaning that it should either increase or stay consistent as the image quality improves. In Fig. 2, the enhancement results of a few thermal images are depicted, showcasing five varying degrees of enhancement. The graphs presented in the same figure display the metric values for different enhancement parameters. It is obvious that LTA, GTA, and LGTA measures exhibit a growth pattern as visibility and contrast in the results improve, thus establishing them as quality metrics with monotonic characteristics.

Although LGTA effectively combines the strengths of LTA and GTA, it is essential to recognize that each component metric exhibits sensitivity to specific distortions. As Table 3 demonstrates, LTA scores tend to increase in the presence of Gaussian noise. At the same time, GTA is more sensitive to significant blur distortions due to its inherent limitations in detecting delicate local structures. The Pearson rank correlation between LTA and GTA is negative in both cases: -0.775 for increasing noise distortion and -0.005 for blur. This indicates an opposite relationship between local and global features under these distortion conditions. Despite these individual sensitivities, LGTA consistently assigns the highest score to the undistorted original image, reinforcing its reliability as a comprehensive image quality assessment metric. Further investigations into the performance of these metrics under various distortion types will be presented in Section 4.

Our proposed approach integrates local and global features to create a robust thermal image quality assessment technique. This method's distinctive strength lies in its ability to emulate the human visual

system's perception by combining global scene understanding with detailed local analysis. This holistic approach enables a more accurate and comprehensive evaluation of thermal images.

4. Results and discussion

4.1. Datasets

Addressing the essential role of datasets in computer simulations and validation, we recognize a notable gap in available datasets for thermal image quality assessments, particularly those with pre-existing image scores for validation and experimentation. Consequently, our methodology involves the careful selection of thermal image datasets, supplemented by an in-depth user study designed to collect the requisite image scores for robust validation. Below, we present the datasets we utilized, providing insights into their specific attributes and relevance to our research objectives.

- *Photovoltaic System Thermal Images* [36]. This dataset comprises 277 thermographic aerial images obtained using a Zenmuse XT IR camera with a $7\text{--}13\ \mu\text{m}$ wavelength, mounted on a DJI Matrice 100 quadcopter drone. In addition to the images, it includes environmental data such as temperature, wind speed, and irradiance.
- *Thermal Image of Equipment* (Induction Motor and Transformer) [37]. This dataset contains thermal images (IRT) to monitor the condition of electrical equipment, specifically Induction Motors and Transformers. The defects present in this dataset are artificially generated internal faults and are not a result of external factors or any failure in the initial setup components. The thermal images were acquired using a Dali-tech T4/T8 infrared thermal image camera at the Electrical Machines Laboratory workbench under an ambient temperature of 23° .
- *The Multi-Spectral Object Detection dataset* [35] consists of multi-spectral images designed for object detection in traffic scenarios. These images encompass RGB, near-infrared, middle-infrared, and far-infrared spectra, offering comprehensive data for detection tasks. The dataset includes objects that might not be visible in RGB images but can be detected in other spectra, such as far-infrared. It was specifically created to train a multispectral object detection system.

These datasets collectively provide a rich and diverse set of thermal imagery for various applications, including photovoltaic system analysis, electrical equipment condition monitoring, and advanced autonomous vehicle research. In our experiments, we utilized these datasets as our primary sources for conducting a user study, generating enhancements, and introducing distortions to evaluate the effectiveness of our thermal metrics.

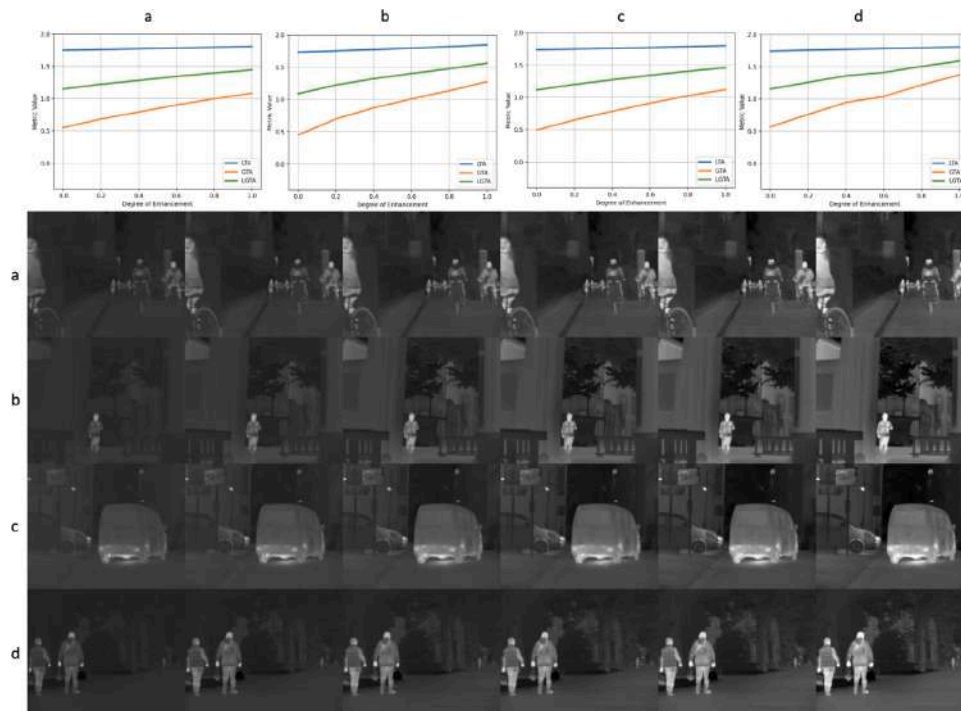


Fig. 2. The proposed metrics consistently ascend with increasing degrees of enhancement.
Source: The images are taken from the dataset described in [35].

Table 3

Ablation study of the LGTA metric. This table presents the performance of LTA, GTA, and LGTA under various distortions, including Poisson noise and box blur. It highlights each metric's specific sensitivities and overall effectiveness, demonstrating the complementary nature of the extracted LTA and GTA features. For example, GTA excels in handling noisy images, while LTA is particularly effective for blurry images. Additionally, the negative Pearson correlation between LTA and GTA (-0.775 for noise and -0.005 for blur) underscores their opposing sensitivities to these distortions. The combined LGTA measure, leveraging the strengths of both LTA and GTA, provides a comprehensive evaluation of thermal image quality.

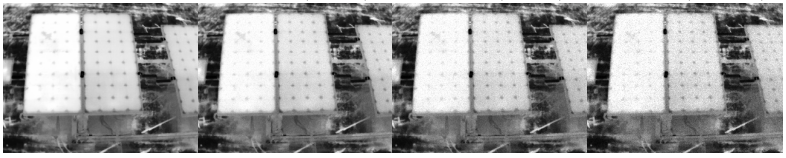
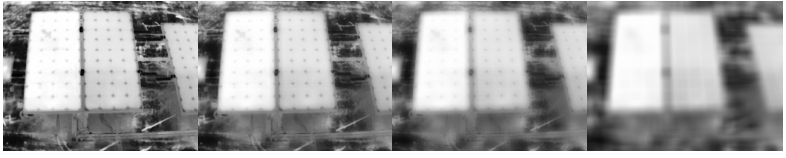
	Source	Noisy (40%)	Noisy (70%)	Noisy (100%)
				
LTA	2.6238	2.6966	2.7560	2.8027
GTA	0.6123	0.2863	0.2855	0.3212
LGTA	1.6181	1.4915	1.5207	1.5620
	Source	Blurry (40%)	Blurry (70%)	Blurry (100%)
				
LTA	2.6238	2.3097	2.1415	2.0472
GTA	0.6123	0.4213	0.5417	0.6316
LGTA	1.6181	1.3655	1.3416	1.3394

Table 4
Average correlations ranks between thermal image quality metrics and user scores.

Metric type	Quality Metric	Kendall rank	Pearson rank
Local	EME	0.510970	0.481541
	DMTE	0.518617	0.549078
	DIMTE	0.478970	0.571109
	MDIMTE	0.471915	0.521113
	BDIM	0.482000	0.570710
	LTA	0.438262	0.448493
Global and Combined	BRISQUE	0.020295	0.105794
	NIQE	0.183993	0.172005
	PIQE	0.067862	-0.026669
	MANIQA	0.094105	0.033886
	TOPIQ	0.293672	0.318487
	GTA	0.702616	0.704283
	LGTA	0.758616	0.730985

4.2. Perceptual validation of proposed metrics based on thermal image enhancement methods

For the user study, we prepared the results of five image enhancement methods (Arici et al. [38], Lee et al. [39], Huang et al. [40], Rahman et al. [41], and Cao et al. [42]) on images three datasets. We selected widely-used histogram and gamma correction-based image enhancement methods that are applicable to both visible and thermal imagery [43]. Our evaluation involved the participation of 20 observers who rated 125 thermal images on a scale of 1 to 5, with 5 representing the most superior enhancement and 1 indicating the least satisfactory outcome. Additionally, the observers were instructed to carefully examine any image distortions following the enhancement process.

To assess the relationship between our newly developed thermal objective metrics and human quality judgments, we employed both Kendall's and Pearson's correlation coefficients. These statistical methods are widely used in image quality assessment to establish correlations between objective metrics and human evaluations [44]. The Pearson correlation coefficient quantifies the linear relationship between an objective metric and human judgments. A high Pearson correlation coefficient signifies that the objective metric is effective at predicting human judgments accurately. In contrast, the Kendall tau rank correlation coefficient assesses the strength and direction of the association between two ranked variables. It focuses on the similarity in the order of observations rather than the specific values, which makes it resilient to non-linear relationships and outliers. These coefficients range from -1 to 1: positive values indicate a direct relationship, negative values suggest an inverse relationship, and zero indicates no monotonic association. Using both Pearson and Kendall correlation coefficients will better understand the relationship between the objective metric and human judgment. The results from both correlation coefficients give a holistic picture. With a high Pearson correlation coefficient, you can ensure that your objective metric has good prediction accuracy. With a high Kendall correlation coefficient, you can ensure that the relationship between the objective metric and human judgment is monotonic.

We collected Mean Opinion Scores (MOS) from all 20 observers for each image under evaluation to further analyze the relationship between the objective metrics and human judgments. MOS is a well-established practice in the IQA of natural images due to its ability to capture human perceptual responses and preferences directly, providing a reliable measure of image quality [45,46]. However, there is a notable lack of established thermal image scores, which prompted us to conduct our experiment. We focus on MOS because it is simple, easy to understand and implement, widely accepted, and used in various fields, making it a standard benchmark [47]. It directly reflects the human perception of quality. On the other hand, Opinion Score Distribution (OSD) provides a more detailed view by showing the distribution of individual ratings rather than just the average, highlighting the

variability and consensus among raters [31]. However, OSD is more complex to analyze and interpret than MOS, requires handling and processing more data points, and may provide more information than necessary for some applications. Therefore, while we plan to use OSD in the future, our current focus remains on MOS due to its simplicity and widespread acceptance.

These subjective scores were then used to calculate the average Kendall and Pearson ranks between the subjective scores and the thermal IQA metrics, detailed in Table 1. The metric calculations were conducted using default parameter values, with a consistent block size of 5 applied to all local metrics. The results of these calculations are presented in Table 4. Given the limited availability of established global feature-based thermal image quality evaluation methods, our primary comparisons are made with widely adopted methods. As anticipated, the NIQE and PIQE metrics exhibited lower correlations with human judgments. These methods, based on statistical and supervised learning approaches, are commonly used for general image quality evaluation, even though they are not explicitly designed for thermal images. Local metrics such as EME, BDIM, and LTA also produced similar results, likely due to their design, which focuses on adjusting parameters only within local blocks of the image. Similarly, MANIQA and TOPIQ, underperform in both metrics compared to our proposed methods, GTA and LGTA. Specifically, the Kendall and Pearson correlation coefficients between the quality metrics and user scores for TOPIQ are 0.29 and 0.32, respectively. In contrast, our proposed LGTA method achieves significantly higher correlations, with Kendall's Tau at approximately 0.76 and Pearson's correlation at 0.73. This notable difference highlights our framework's ability to align with human subjective quality assessments more accurately and provides practical insights for improving thermal image quality evaluation. The values of proposed metrics and user ranking on five enhanced images are shown in Table 5. In terms of monotonicity, all three metrics exhibit strong correlations with user ranks in the first example. However, in the second example, LTA has a higher Kendall rank than GTA and LGTA. This discrepancy might stem from relatively imprecise user rankings, mainly since the visual outcomes are similar.

4.3. Qualitative evaluation of proposed metrics using different thermal image distortions

In this section, we assess the proposed metrics by applying them to a range of distorted thermal images. Building upon the approach of Li et al. [48], we generate a diverse set of distortion scenarios, including Salt and Pepper, Gaussian, Poisson, and Blurring, and analyze how our metrics perform under these conditions. Detailed descriptions of the experiments and results are provided below.

- **Salt and Pepper Noise:** This noise introduces randomly isolated dark and bright pixels into thermal images, which can occur due to sensor limitations or environmental factors in thermal imaging. We vary the noise density from 0.01 to 0.1 and employ our metrics to measure the quality scores of the distorted images.
- **Gaussian Noise:** Gaussian noise simulates the noise commonly encountered in thermal images, often originating from sensor imperfections or electronic interference.
- **Poisson Noise:** We apply Poisson noise to the images to replicate the inherent variability in the number of photons detected in thermal imaging. This noise is particularly relevant for simulating low-light conditions.
- **Blur:** Introduces a form of distortion, whether through Gaussian or Box blurring, which can result from various factors such as motion or defocusing during image capture. This encompasses common scenarios in thermal imaging where blurring effects may arise due to real-world conditions and imaging challenges.

Table 5

User scores and LGTA values for several thermal image enhancement methods. LGTA is calculated with different values of α and β parameters [38–42].

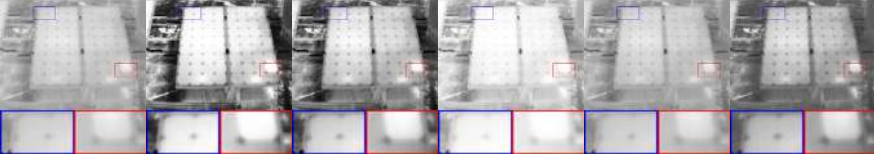

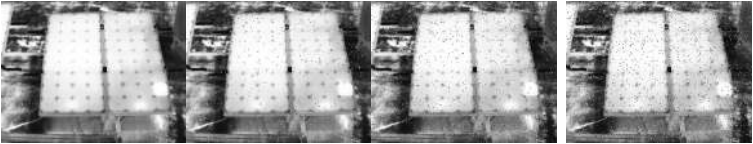
Source Image	Arici [38]	Lee [39]	Huang [40]	Rahman [41]	Cao [42]
					
LGTA/Score	5	4	1	2	3
$\alpha=1, \beta=0$ (LTA)	1.9276	1.8945	1.7741	1.7717	1.8068
$\alpha=0, \beta=1$ (GTA)	0.6151	0.5054	0.3800	0.3222	0.5108
$\alpha=0.5, \beta=0.5$	1.2714	1.2000	1.071	1.0470	1.1588
$\alpha=0.2, \beta=0.8$	0.8776	0.7832	0.6588	0.6121	0.7700
$\alpha=0.7, \beta=0.3$	1.5339	1.4778	1.3559	1.3368	1.4180
					
LGTA/Score	4	5	3	1	2
$\alpha=1, \beta=0$ (LTA)	1.802	1.8032	1.7726	1.7702	1.7785
$\alpha=0, \beta=1$ (GTA)	1.7848	2.1435	2.0309	1.7648	2.3299
$\alpha=0.5, \beta=0.5$	1.7934	1.9733	1.9017	1.7675	2.0542
$\alpha=0.2, \beta=0.8$	1.7882	2.0754	1.9792	1.7659	2.2196
$\alpha=0.7, \beta=0.3$	1.7968	1.9053	1.8501	1.7686	1.9439

Table 6

Different metric values for artificially generated four levels of salt and pepper noise.

				
Noise density	0	0.05	0.1	0.2
DIMTE*	0.0643	0.0548	0.0471	0.0388
BDIM	0.9411	0.9498	0.9569	0.9644
MANIQA	0.3287	0.4545	0.4936	0.4116
TOPIQ	0.3265	0.4323	0.4034	0.3985
LTA	1.9276	1.9195	1.9090	1.8895
GTA	0.6151	0.5080	0.4403	0.3893
LGTA	1.2714	1.2137	1.1746	1.1394

*Lower scores for certain metrics (DMTE, DIMTE, etc.) indicate better quality.

For each type of distortion, we systematically corrupted a subset of the thermal images in our dataset at varying noise levels. These distorted images were then evaluated using our proposed metrics, along with state-of-the-art ones like BDIM and DMTE, for comparison. The objective was to observe how well the metrics could assess the image quality in the presence of these specific distortions.

Table 6 presents a set of four distinct thermal images, each exemplifying a different level of Salt and Pepper noise, spanning from minimal noise to severe distortion. These visual examples effectively depict the diverse noise levels applied to the thermal images. We observed that: the LGTA metric consistently demonstrated robustness and

accuracy across all types of distortions, showing a consistent decrease as the level of distortion increases. In contrast, established metrics such as BDIM, DMTE, and MANIQA displayed limitations in effectively assessing image quality under certain distortion types.

Fig. 3 illustrates how our proposed LGTA metric responds to increasing distortion density across various distortion types, including noises and blurring. The consistent trend observed with our metric is noteworthy. As the distortion density intensifies in thermal images, LGTA demonstrates the highest correlation, consistently decreasing. This pattern underscores its exceptional sensitivity in evaluating thermal image quality amidst rising distortion levels, emphasizing its practical utility in challenging conditions.

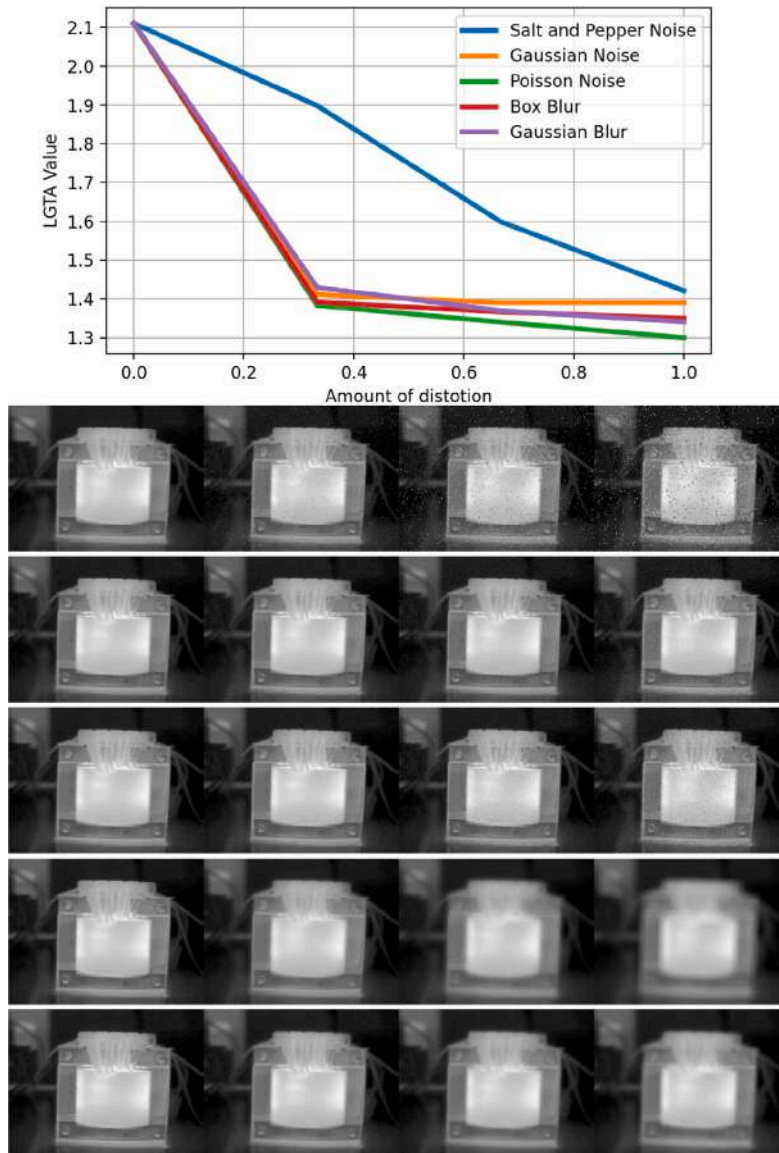


Fig. 3. The behavior of the proposed LGTA metric under varying degrees of distortions.

4.4. LGTA-based thermal image enhancement

In addition to assessing thermal image quality and selecting optimal enhancement methods, quality metrics are valuable for optimizing parameters in simple algorithms. We employed the novel LGTA method and Genetic Algorithms to optimize CLAHE parameters to enhance thermal image quality [49]. The optimization steps are described in Algorithm 1. Fig. 4 illustrates the outcomes of this optimization process on solar panel images. We utilized a grid size of (3, 3) and optimized the 'clip limit' parameter within the range [0, 50]. The enhanced images clearly show that hot spot defects on panels are much more visible, which can be beneficial for defect detection algorithms and thermal dataset augmentation.

5. Conclusion

In this paper, we presented a novel method for assessing the quality of thermal images, addressing the unique challenges posed by infrared

thermal imaging technology. Inspired by the human vision system, our approach harmonizes local and global data to deliver accurate image quality predictions without the need for reference images. The primary contributions of this work include the development of innovative local, global, and hybrid thermal quality assessment methods, an experimental analysis of the blind thermal IQA measure's applicability to solar panel images, and a comprehensive evaluation of traditional IQA methods applied to publicly accessible thermal image databases. Our extensive computer simulations demonstrated that our method outperforms state-of-the-art approaches and closely aligns with human perception of image quality. By investigating the correlation between our quality assessments and human ratings, we showcased the efficacy of our approach. These methods are valuable for evaluating and optimizing thermal imaging systems and comparing different image processing algorithms regarding their impact on image fidelity and utility.

Future work will extend the proposed methods to other thermal quality measures and imaging applications, such as image enhancement, segmentation, and fault detection. Using the proposed thermal

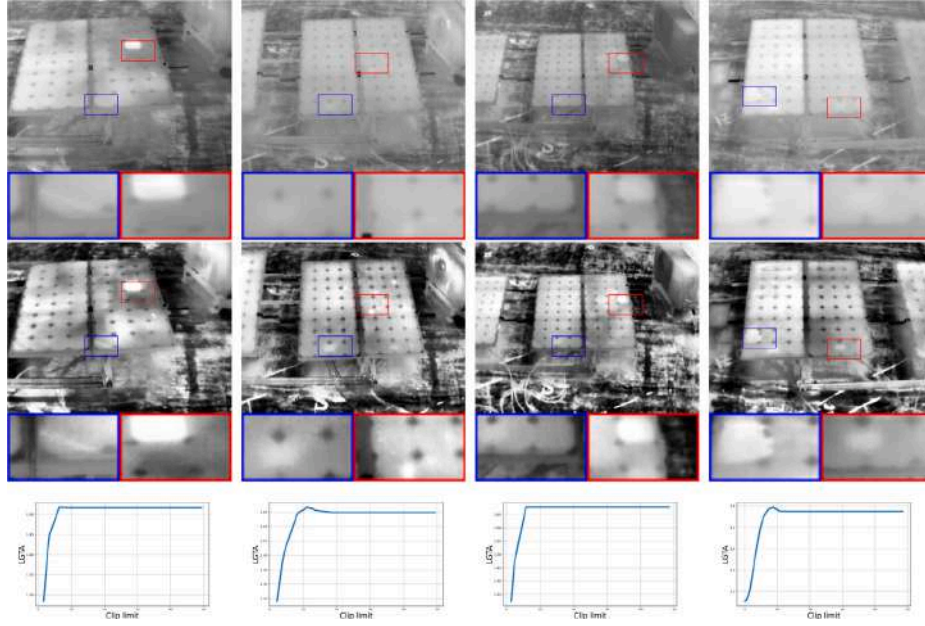


Fig. 4. Optimal enhancement of thermal images using the LGTA metric and CLAHE method. The first row displays the source images, their enhanced versions are shown in the second row, and optimization graphs are displayed in the third one.

Algorithm 1 Optimal thermal image enhancement using Genetic Algorithm with a novel cost function

Inputs: I_s = source image
Initialization: population = n , maximum number of iterations = N , $t = 0$
Function objective(p_1, \dots, p_n)
 $I_e = \text{Enhance}(p_1, \dots, p_n)$
 $m = \text{CalculateLGTA}(I_e)$
return m
EndFunction
Generate the initial number of n chromosomes
Compute the fitness of each chromosome using the objective function
while $t < N$ **do**
 Select a pair of chromosomes based on fitness
 Apply crossover on the selected pair
 Apply mutation operation
 Replace the old population with the newly generated one
 $t \leftarrow t + 1$
end while
Return parameters with the best fitness
Output: p_1, \dots, p_n parameters

image quality measurement, we plan to develop an efficient method to display only the temperature range of electrical equipment's infrared thermal images. This will improve the accuracy and reliability of tasks in energy-related imaging scenarios. Additionally, we will conduct experiments on multispectral thermal images and diverse datasets to comprehensively evaluate the proposed methods and their applicability in various settings. Furthermore, we plan to focus on UAV imaging applications in critical areas such as volcanism, detecting temperature changes as potential indicators for forecasting future events, and inspecting industrial electromechanical elements. These applications can play a crucial role in preventing system malfunctions and improving safety and reliability.

CRedit authorship contribution statement

Sos Aghaian: Writing – review & editing, Writing – original draft, Supervision, Project administration, Methodology, Investigation, Funding acquisition, Conceptualization. **Hrach Ayunts:** Writing – review & editing, Writing – original draft, Visualization, Validation, Software, Resources, Methodology. **Thaweesak Trongtirakul:** Methodology, Investigation, Formal analysis, Conceptualization. **Sargis Hovhannisyan:** Visualization, Validation, Resources.

Declaration of competing interest

The authors declare the following financial interests/personal relationships which may be considered as potential competing interests: Hrach Ayunts reports financial support was provided by Foundation for Armenian Science and Technology. Sargis Hovhannisyan reports financial support was provided by Foundation for Armenian Science and Technology. If there are other authors, they declare that they have no known competing financial interests or personal relationships that could have appeared to influence the work reported in this paper.

Acknowledgment

The research is conducted within the ADVANCE Research Grant provided by the Foundation for Armenian Science and Technology funded by Sarkis and Nune Sepetjians.

Data availability

Data will be made available on request.

References

- [1] R. Roslidar, A. Rahman, R. Muharar, M.R. Syahputra, F. Arnia, M. Syukri, B. Pradhan, K. Munadi, A review on recent progress in thermal imaging and deep learning approaches for breast cancer detection, *IEEE Access* 8 (2020) 116176–116194.
- [2] L. Bezerra, M. Oliveira, T. Rolim, A. Conci, F. Santos, P.R.M. Lyra, R.C. Lima, Estimation of breast tumor thermal properties using infrared images, *Signal Process.* 93 (10) (2013) 2851–2863.
- [3] Q. Liu, Z. He, X. Li, Y. Zheng, PTB-TIR: A thermal infrared pedestrian tracking benchmark, *IEEE Trans. Multimed.* 22 (3) (2019) 666–675.
- [4] V. Singh, N. Sharma, S. Singh, A review of imaging techniques for plant disease detection, *Artif. Intell. Agric.* 4 (2020) 229–242.
- [5] Y. Wang, B. Gao, W. Lok Woo, G. Tian, X. Maldague, L. Zheng, Z. Guo, Y. Zhu, Thermal pattern contrast diagnostic of microcracks with induction thermography for aircraft braking components, *IEEE Trans. Ind. Inform.* 14 (12) (2018) 5563–5574.
- [6] M. Roopaei, S. Agaian, M. Jamshidi, Thermal imaging in fuzzy condition monitoring, in: 2014 World Automation Congress, WAC, IEEE, 2014, pp. 593–597.
- [7] Q. Liu, X. Li, Z. He, N. Fan, D. Yuan, H. Wang, Learning deep multi-level similarity for thermal infrared object tracking, *IEEE Trans. Multimed.* 23 (2020) 2114–2126.
- [8] C. Schuss, K. Remes, K. Leppänen, J. Saarela, T. Fabritius, B. Eichberger, T. Rahkonen, Detecting defects in photovoltaic panels with the help of synchronized thermography, *IEEE Trans. Instrum. Meas.* 67 (5) (2018) 1178–1186.
- [9] Y. Lin, C. Li, Y. Yang, J. Qin, X. Su, H. Zhang, W. Zhang, Automatic display temperature range adjustment for electrical equipment infrared thermal images, *Energy Procedia* 141 (2017) 454–459.
- [10] W. Zhou, X. Lin, J. Lei, L. Yu, J.-N. Hwang, MFFNet: Multiscale feature fusion and enhancement network for RGB-thermal urban road scene parsing, *IEEE Trans. Multimed.* 24 (2021) 2526–2538.
- [11] F. Amon, A. Lock, Evaluation of Image Quality of Thermal Imagers Used by the Fire Service, US Department of Commerce, National Institute of Standards and Technology, 2009.
- [12] K. Panetta, C. Gao, S. Agaian, No reference color image contrast and quality measures, *IEEE Trans. Consum. Electron.* 59 (3) (2013) 643–651.
- [13] X. Min, K. Gu, G. Zhai, J. Liu, X. Yang, C.W. Chen, Blind quality assessment based on pseudo-reference image, *IEEE Trans. Multimed.* 20 (8) (2017) 2049–2062.
- [14] X. Min, G. Zhai, K. Gu, Y. Liu, X. Yang, Blind image quality estimation via distortion aggravation, *IEEE Trans. Broadcast.* 64 (2) (2018) 508–517.
- [15] M. Hu, G. Zhai, R. Xie, X. Min, Q. Li, X. Yang, W. Zhang, A wavelet-predominant algorithm can evaluate quality of THz security image and identify its usability, *IEEE Trans. Broadcast.* 66 (1) (2019) 140–152.
- [16] X. Min, Y. Gao, Y. Cao, G. Zhai, W. Zhang, H. Sun, C.W. Chen, Exploring rich subjective quality information for image quality assessment in the wild, 2024, arXiv preprint [arXiv:2409.05540](https://arxiv.org/abs/2409.05540).
- [17] X. Min, H. Duan, W. Sun, Y. Zhu, G. Zhai, Perceptual video quality assessment: A survey, 2024, arXiv preprint [arXiv:2402.03413](https://arxiv.org/abs/2402.03413).
- [18] J. Liu, W. Zhou, X. Li, J. Xu, Z. Chen, LIQA: Lifelong blind image quality assessment, *IEEE Trans. Multimed.* (2022).
- [19] Y. Cao, X. Min, W. Sun, G. Zhai, Attention-guided neural networks for full-reference and no-reference audio-visual quality assessment, *IEEE Trans. Image Process.* 32 (2023) 1882–1896.
- [20] A. Mittal, A.K. Moorthy, A.C. Bovik, No-reference image quality assessment in the spatial domain, *IEEE Trans. Image Process.* 21 (12) (2012) 4695–4708.
- [21] A. Mittal, R. Soundararajan, A.C. Bovik, Making a “completely blind” image quality analyzer, *IEEE Signal Process. Lett.* 20 (3) (2012) 209–212.
- [22] N. Venkatanath, D. Praneeth, M.C. Bh, S.S. Channappayya, S.S. Medasani, Blind image quality evaluation using perception based features, in: 2015 Twenty First National Conference on Communications, NCC, IEEE, 2015, pp. 1–6.
- [23] T.R. Goodall, A.C. Bovik, N.G. Paulter, Tasking on natural statistics of infrared images, *IEEE Trans. Image Process.* 25 (1) (2015) 65–79.
- [24] S. Yang, T. Wu, S. Shi, S. Lao, Y. Gong, M. Cao, J. Wang, Y. Yang, Maniqa: Multi-dimension attention network for no-reference image quality assessment, in: Proceedings of the IEEE/CVF Conference on Computer Vision and Pattern Recognition, 2022, pp. 1191–1200.
- [25] C. Chen, J. Mo, J. Hou, H. Wu, L. Liao, W. Sun, Q. Yan, W. Lin, Topiq: A top-down approach from semantics to distortions for image quality assessment, *IEEE Trans. Image Process.* (2024).
- [26] S.S. Agaian, K. Panetta, A.M. Grigoryan, A new measure of image enhancement, in: IASTED International Conference on Signal Processing & Communication, Citeseer, 2000, pp. 19–22.
- [27] S. Agaian, M. Roopaei, D. Akopian, Thermal-image quality measurements, in: 2014 IEEE International Conference on Acoustics, Speech and Signal Processing, ICASSP, IEEE, 2014, pp. 2779–2783.
- [28] T. Trongtirakul, S. Agaian, Unsupervised and optimized thermal image quality enhancement and visual surveillance applications, *Signal Process., Image Commun.* 105 (2022) 116714.
- [29] G. Zhai, X. Min, Perceptual image quality assessment: a survey, *Sci. China Inf. Sci.* 63 (2020) 1–52.
- [30] X. Min, K. Gu, G. Zhai, X. Yang, W. Zhang, P. Le Callet, C.W. Chen, Screen content quality assessment: Overview, benchmark, and beyond, *ACM Comput. Surv.* 54 (9) (2021) 1–36.
- [31] Y. Gao, X. Min, Y. Zhu, J. Li, X.-P. Zhang, G. Zhai, Image quality assessment: From mean opinion score to opinion score distribution, in: Proceedings of the 30th ACM International Conference on Multimedia, 2022, pp. 997–1005.
- [32] Y. Gao, X. Min, Y. Zhu, X.-P. Zhang, G. Zhai, Blind image quality assessment: A fuzzy neural network for opinion score distribution prediction, *IEEE Trans. Circuits Syst. Video Technol.* (2023).
- [33] S. Budzan, R. Wyżgolik, Noise reduction in thermal images, in: International Conference on Computer Vision and Graphics, Springer, 2014, pp. 116–123.
- [34] S.S. Agaian, Visual morphology, in: Nonlinear Image Processing X, Vol. 3646, SPIE, 1999, pp. 139–150.
- [35] K. Takumi, K. Watanabe, Q. Ha, A. Tejero-De-Pablos, Y. Ushiku, T. Harada, Multispectral object detection for autonomous vehicles, in: Proceedings of the on Thematic Workshops of ACM Multimedia 2017, 2017, pp. 35–43.
- [36] E. Mejia, H.L. Correa, E. Mejia, R. Girón, A. David, N. Rodriguez, S. Esperanza, Photovoltaic system thermal images, 2019, Mendeley Data: Amsterdam, the Netherlands.
- [37] M. Najafi, Y. Baleghi, S.A. Gholamian, S.M. Mirimani, Fault diagnosis of electrical equipment through thermal imaging and interpretable machine learning applied on a newly-introduced dataset, in: 2020 6th Iranian Conference on Signal Processing and Intelligent Systems, ICSPIS, IEEE, 2020, pp. 1–7.
- [38] T. Arici, S. Dikbas, Y. Altunbasak, A histogram modification framework and its application for image contrast enhancement, *IEEE Trans. Image Process.* 18 (9) (2009) 1921–1935.
- [39] C. Lee, C. Lee, C.-S. Kim, Contrast enhancement based on layered difference representation of 2D histograms, *IEEE Trans. Image Process.* 22 (12) (2013) 5372–5384.
- [40] S.-C. Huang, F.-C. Cheng, Y.-S. Chiu, Efficient contrast enhancement using adaptive gamma correction with weighting distribution, *IEEE Trans. Image Process.* 22 (3) (2012) 1032–1041.
- [41] S. Rahman, M.M. Rahman, M. Abdullah-Al-Wadud, G.D. Al-Quaderi, M. Shoyaib, An adaptive gamma correction for image enhancement, *EURASIP J. Image Video Process.* 2016 (1) (2016) 1–13.
- [42] G. Cao, L. Huang, H. Tian, X. Huang, Y. Wang, R. Zhi, Contrast enhancement of brightness-distorted images by improved adaptive gamma correction, *Comput. Electr. Eng.* 66 (2018) 569–582.
- [43] R. Soundrapandiyan, S.C. Satapathy, C.M. PVSSR, N.G. Nhu, A comprehensive survey on image enhancement techniques with special emphasis on infrared images, *Multimedia Tools Appl.* 81 (7) (2022) 9045–9077.
- [44] S. Mukherjee, G. Valenzise, I. Cheng, Potential of deep features for opinion-unaware, distortion-unaware, no-reference image quality assessment, in: International Conference on Smart Multimedia, Springer, 2019, pp. 87–95.
- [45] N. Ponomarenko, O. Ieremeiev, V. Lukin, L. Jin, K. Egiazarian, J. Astola, B. Vozel, K. Chehdi, M. Carli, F. Battisti, et al., A new color image database TID2013: Innovations and results, in: Advanced Concepts for Intelligent Vision Systems: 15th International Conference, ACIVS 2013, Poznań, Poland, October 28–31, 2013. Proceedings 15, Springer, 2013, pp. 402–413.
- [46] S. Pandey, D. Sharma, B. Kumar, H. Singh, Quality assessment of deep learning based super resolution techniques on thermal images, in: 2021 IEEE 18th India Council International Conference, INDICON, IEEE, 2021, pp. 1–6.
- [47] R.C. Streijl, S. Winkler, D.S. Hands, Mean opinion score (MOS) revisited: methods and applications, limitations and alternatives, *Multimedia Syst.* 22 (2) (2016) 213–227.
- [48] Y. Li, X. Ye, Y. Li, Image quality assessment using deep convolutional networks, *AIP Adv.* 7 (12) (2017).
- [49] S.K. Pal, D. Bhandari, M.K. Kundu, Genetic algorithms for optimal image enhancement, *Pattern Recognit. Lett.* 15 (3) (1994) 261–271.